

Document downloaded from:

<http://hdl.handle.net/10251/144582>

This paper must be cited as:

Cobos, CM.; Garzón, L.; López-Martínez, J.; Fenollar, O.; Ferrándiz Bou, S. (13-0). Study of thermal and rheological properties of PLA loaded with carbon and halloysite nanotubes for additive manufacturing. *Rapid Prototyping Journal*. 25(4):738-743.  
<https://doi.org/10.1108/RPJ-11-2018-0289>



The final publication is available at

<https://doi.org/10.1108/RPJ-11-2018-0289>

Copyright Emerald

Additional Information

1           **Study of thermal and rheological properties of PLA loaded with carbon and**  
2                                   **halloysite nanotubes for additive manufacturing**

3   **PURPOSE:**

4   This paper proposes using polylactic acid (PLA) as an alternative to nanocomposites in  
5   additive manufacturing processes in Fusion Deposition Modelling (FDM) systems and  
6   describes its thermal and rheological conditions with multiwall carbon nanotubes  
7   (PLA/MWCNTs) and halloysite nanotubes (PLA/HNTs) composites for possible  
8   applications in additive manufacturing processes.

9   **DESIGN/METHODOLOGY/APPROACH**

10   PLA/MWCNTs and PLA/HNTs were obtained through fusion in a co-rotating twin-  
11   screw extruder. PLA was mixed with different percentages of MWCNTs and HNTs at  
12   concentrations of 0.5 wt. %, 0.75wt. %, and 1wt. %. Differential Scanning Calorimetry  
13   (DSC) and Capillary Rheometry were used to characterise these products, together with  
14   an analysis of the Melt Flow Index (MFI).

15   **FINDING:**

16   The DSC data revealed that the nanocomposites had a glass transition temperature  $T_g =$   
17    $65 \pm 2^\circ\text{C}$  and a melting temperature  $T_m = 169 \pm 1^\circ\text{C}$ .

18   The crystallisation temperature of PLA/MWCNTs and PLA/HNTs was between  $107 \pm$   
19    $2^\circ\text{C}$ , and  $129^\circ\text{C}$ , respectively. The PLA / MWCNTs and PLA / HNTs viscosity data  
20   obtained by capillary rheometry indicated that the viscosity of the materials is the same  
21   as that of neat PLA.

22   These results were confirmed by the higher fluidity index in the MFI analysis.

23   **Originality /value:**

24   This paper presents an alternative for the applications of nanocomposites in additive  
25   manufacturing processes in Fusion Deposition Modeling (FDM) systems.

26 **KEYWORDS:** 3D printing, additive manufacturing, carbon nanotubes, halloysite  
27 nanotubes, thermal, rheological.

## 28 **INTRODUCTION**

29 PLA, a natural biopolymer, is now becoming an alternative to diminishing oil resources  
30 for use in FDM processes. Although PLA has good mechanical properties, it also has  
31 certain disadvantages, such as low thermal resistance and low shear and crystallization  
32 rates, however there are different PLA nanocomposites that use different mixing  
33 methods (Raquez *et al.*, 2013).

34 As PLA is biodegradable, research groups all over the world are studying how to apply  
35 it to polymer transformation processes for different uses(Auras *et al.*, 2011).

36 Natural biodegradable polymers and synthetic polymers based on renewable materials  
37 are the basis for the sustainable development of new eco-efficient plastics(Auras *et al.*,  
38 2011).

39 While lactic acid is the most frequently occurring natural carboxylic acid, PLA is a  
40 thermoplastic with similar stiffness to polyethylene (PE) or ethyl poly terephthalate  
41 (PET) (Auras *et al.*, 2011)(Ren, 2011).

42 PLA has been tested for possible use in injection and additive manufacturing processes.  
43 Its rheological, mechanical and thermal characteristics have been analysed in order to  
44 determine the agents that improve its properties for manufacturing by injection. Studies  
45 have also been made on applying PLA to fused deposition modelling (FDM) to  
46 determine suitable strategies to improve the mechanical characteristics of components  
47 obtained by additive manufacturing (Harris and Lee, 2008)(Song *et al.*, 2017).

48 Carbon nanotubes (CNTs) and halloysite nanotubes in a PLA polymer matrix create a  
49 class of novel materials with a wide range of characteristics and applications.

50 HNTs are derived from clay. Halloysite is formed by the weathering of different types  
51 of igneous and non-igneous rock (Yuan, Tan and Annabi-Bergaya, 2015) and is  
52 chemically similar to kaolinite, except that halloysite unit layers are separated by a  
53 nanowire of water droplets

54 Carbon nanotubes are cylindrical structures between ten and fifty thousand times  
55 thinner than a hair, with ends may be either open or closed by a hemispherical cap,  
56 while they can reach a macroscopic scale in length (Angel Herráez, 2011).

57 The aim of this work was to determine the influence of carbon nanotubes and halloysite  
58 nanotubes on a PLA polymer matrix and to analyse the thermal properties and rheology  
59 of the nanocomposites obtained for use in additive manufacturing. The halloysite nano  
60 compound is designed for use in the regenerative medicine and pharmaceutical science  
61 fields.

62 The nanocomposite consisting of materials based on multi wall carbon nanotubes is  
63 aimed at FDM 3D component printing applications.

## 64 **MATERIAL AND METHODS**

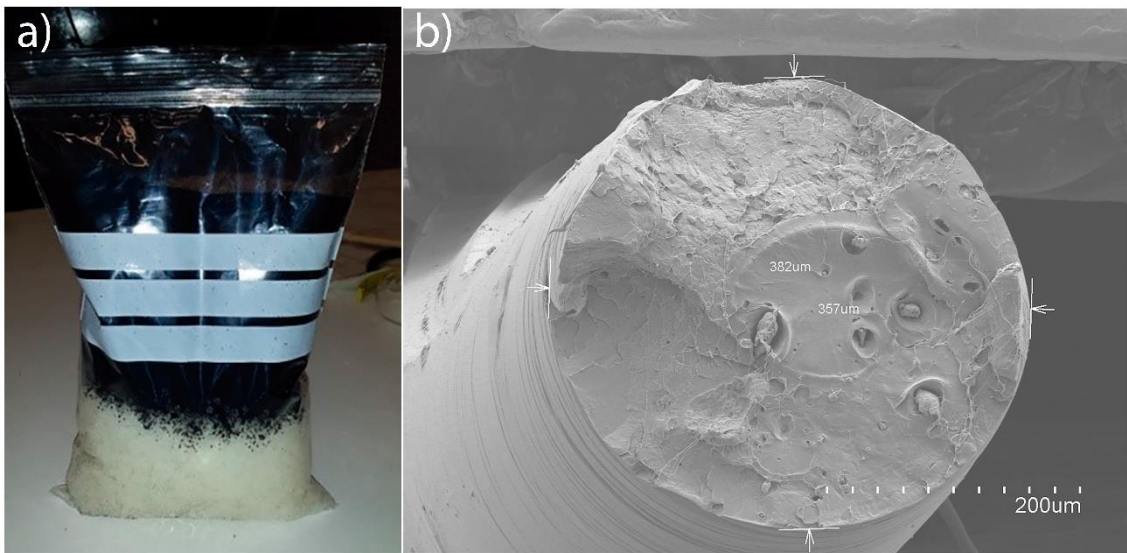
### 65 *MATERIALS*

66 PLA (lactic acid) was supplied by Ingeo <sup>TM</sup> Biopolymer 6201D, of Nature Works  
67 (Minnetonka, Minnesota, USA) and was used as matrix for nanocomposites made from  
68 PLA/MWCNTs and PLA/HNTs.

69 NC 7000 multi-wall carbon nanotube was supplied by NANOCYL (Sambreville,  
70 Belgium) and halloysite nanotube was obtained from SIGMA – ALDRICH (Darmstadt,  
71 Germany).

### 72 *NANOCOMPOSITE PRODUCTION*

73 In order to avoid degradation by hydrolysis(Murariu and Dubois, 2016)(Carrasco *et al.*,  
74 2010), before extrusion the material was dried in a G-ESN Series PIOVAN hot air dryer  
75 from Nature Works (Minnetonka, Minnesota, USA) at temperatures between 45 and 60  
76 ° C for 8 hours.  
77 For each nanocomposite mix, 0.5%, 0.75% and 1% by weight of multi wall carbon  
78 nanotubes (figure 1a) and halloysite nanotubes, respectively, were added to 1 kilo of  
79 PLA. The mixes were then homogenised in a vibrating drum before extrusion. Figure 1b  
80 show a SEM image of PLA/MWCNTs filament obtained from 3D printer.



81

82 Figure 1: a) PLA + MWCNTs before mixing.

83 b) SEM of 0.5% wt. PLA/MWCNT filament obtained from 3D printer.

84 PLA / MWCNTs and PLA / HNTs nanocomposites were prepared by the direct melt  
85 method, and the materials were mixed in a co-rotating twin-screw extruder (DUPRA),  
86 with a screw diameter of 30 mm and L / D ratio = 20 and turning speed at 40 RPM.

87 The temperature profile of the four controllers ranged between 190, 195, 200 and 205 °  
88 C.

89 Prior to thermal and rheological characterisation, the composites were dried at 60  
90 degrees for 8 hours.

## 91 **NANOCOMPOSITES CHARACTERIZATION**

### 92 *Differential scanning calorimetry (DSC)*

93 To determine any changes in the T<sub>g</sub> transition melting temperatures of the materials  
94 containing different percentages of MWCNTs and HNTs and the amount of heat  
95 absorbed or released at a constant temperature for a given period of time (Suriñach *et*  
96 *al.*, 1992)(Richard, 2008), the thermal properties of the samples were studied by a DSC  
97 calorimeter (Mettler-Toledo 821), with a temperature program of 30 to 350 °C at 10 °C /  
98 min in a nitrogen atmosphere of 66 ml, in accordance with ISO\_11357-1 and  
99 ISO\_11357-3.

### 100 *Capillary Rheometry Testing*

101 Capillary rheometry can identify shear viscosity, which is the primary measure of flow  
102 resistance, and thus affects the actual processes, especially under changes in  
103 temperature and flow rate. The Cross-WFL model was used to fit the curves.  
104 For the tests, a capillary rheometer was used (Malvern Instruments Model RH2000)  
105 according to the ASTM 3835-10.

### 106 *Melt Flow Index (MFI)*

107 A Melt Flow Tester (INDEXER MFI 3000 Series QUALITEST) was used to measure  
108 the flow of a thermoplastic polymer, defined as the weight in grams that flows through a  
109 capillary tube of a specific diameter and length in 10 minutes at a temperature of 210  
110 °C, in accordance with ISO 1133.

## 111 **RESULTS AND DISCUSSION**

### 112 *Differential scanning calorimetry (DSC)*

113 Figure 2 compares the DSC curves of neat PLA and the different percentages of PLA  
114 with MWCNT nanocomposites. The values of their thermal properties are given in  
115 Table 1.

116 **Table1: PLA thermal parameters with different MWCNT concentrations obtained**  
 117 **by differential scanning calorimetry (DSC).**

MWCNTs (%)	PLA/MWCNTs Thermal Properties			
	T <sub>g</sub> (°C)	T <sub>cc</sub> (°C)	T <sub>m</sub> (°C)	T <sub>d</sub> (°C)
<b>0</b>	64.33	105.55	170.69	328.19
<b>0.5</b>	63.86	105.45	171.53	322
<b>0.75</b>	64.74	108.26	171.87	329.78
<b>1</b>	64.41	105.14	170.90	325.12

118

119 The neat PLA DSC curves (Curve 2a) and those of PLA nanocomposites with 0.5 wt.%,  
 120 0.75 wt.% and 1 wt.% MWCNT (2a, 2b, 2c, 2d, respectively) show that the glass  
 121 transition temperature is T<sub>g</sub> = 64.22°C (2a) , T<sub>g</sub> = 63.86°C(2b), T<sub>g</sub> = 64.74°C(2c) and  
 122 T<sub>g</sub> = 64.41°C (2d), in agreement with the findings of Y. Gao, O. T. Picot, E. Bilotti and  
 123 Peijs (Gao *et al.*, 2017).

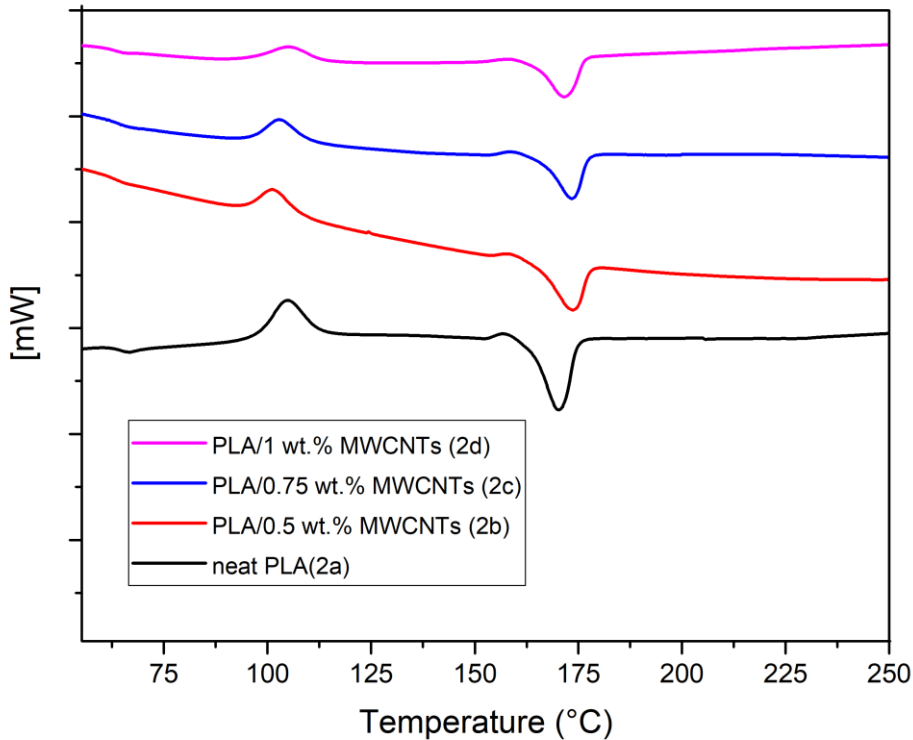
124 In the neat PLA curve (2a) exothermic peak of the crystallization temperature is present,  
 125 however, the endothermic peak T<sub>m</sub> = 169.81°C gives the melt temperature and the  
 126 material's degradation temperature, T<sub>d</sub> = 325.26°C.

127 Temperature is a crucial parameter in the crystallization process, both for production  
 128 and the manufacture of products (López *et al.*, 2009).

129 In Figure 2, in the thermograms of PLA / 0.5%, 0.75%, and 1% MWCNT,  
 130 crystallisation peaks can be seen during the DSC cycle of the nanocomposites,  
 131 indicating that the PLA polymer chains did not crystallise completely. The  
 132 crystallisation temperatures were 105.45°C, 108.26°C and 105.14°C, respectively.

133

134



135

136

**Figure2. DSC (melting temperature peaks) of PLA / MWCNT nanocomposites and neat PLA.**

137

138 Neither fusion temperature nor melting temperature differed significantly from the neat  
 139 PLA. As be seen in Table 1, the melting temperature ( $T_m$ ) for neat PLA is 169.81 °C,  
 140 that of PLA / 0.5 wt.% MWCNT is 171.53 °C, PLA / 0.75wt.% MWCNTs is 171.87 °C  
 141 and PLA / 1% MWCNTs is 170.90 °C. The difference between the melting temperature  
 142 of PLA nanocomposites and MWCNTs is 2 ° C, indicating that carbon nanotubes do not  
 143 influence the processing temperature.

144 The degradation temperature of the PLA / MWCNT nanocomposites and neat PLA  
 145 oscillates between 322 and 325.12 °C, due to PLA degradation after the rupture of the  
 146 polymer chains and the loss of hydrogen (Kim *et al.*, 2010).

147 Figure 3 gives the comparative curves of neat PLA DSC and PLA nanocomposites with  
 148 halloysite nanotubes. Their thermal properties can be seen in Table 2.



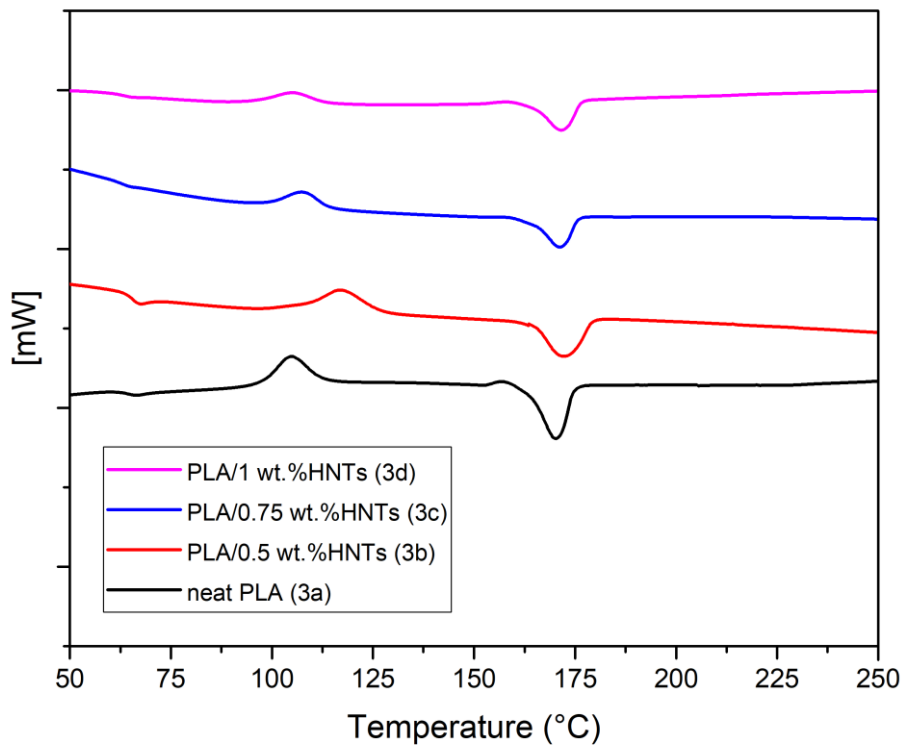
149 **Table 2: Thermal parameters of PLA at different HNTs concentrations obtained**  
 150 **by differential scanning calorimetry (DSC).**

HNTs (%)	PLA/HNTs Thermal Properties			
	T <sub>g</sub> (°C)	T <sub>cc</sub> (°C)	T <sub>m</sub> (°C)	T <sub>d</sub> (°C)
<b>0</b>	64.33	105.55	170.69	328.19
<b>0.5</b>	64.81	129.23	171	318.51
<b>0.75</b>	65.62	129.01	170.87	323.06
<b>1</b>	65.77	129.91	171.02	326.44

151

152 In the DSC curves of PLA nanocomposites with 0.5 wt.%, 0.75 wt.% and 1 wt.% HNT  
 153 (3b, 3c, 3d, respectively) and neat PLA (3a), the glass transition temperature is  
 154 T<sub>g</sub>=64.20°C, T<sub>g</sub>=64.81°C, T<sub>g</sub>=65.62°C, T<sub>g</sub>=65.77°C. These results are similar to the  
 155 glass transition temperature of the DSC curves of PLA/MWCNTs nanocomposites (see  
 156 Table 1) and agree with previous findings (Gao *et al.*, 2017)(Wu *et al.*, 2013).

157



158

159  
160  
161

**Figure 3. DSC (melting temperature peaks) of PLA / HNT nanocomposites**

162

**and neat PLA.**

163 The neat PLA curve (3a) shows an exothermic peak crystallisation temperature,  
164 although there is an endothermic peak for the melting temperature,  $T_m=169.81^\circ\text{C}$ . The  
165 degradation temperature of the material is  $T_d=319.15^\circ\text{C}$ .

166 As can be seen in Table 2, the crystallisation temperature obtained in the different PLA /  
167 HNT nanocomposite tests is  $129^\circ\text{C}$ , or  $24^\circ\text{C}$  higher than the PLA / CNT  
168 nanocomposites. This variation is due to difference in the coefficient of thermal  
169 conductivity.

170 The melting temperature of PLA / HNT nanocomposites is  $170 \pm 2^\circ\text{C}$ , similar to that of  
171 the PLA / MWCNT compounds, indicating that the halloysite nanotubes do not  
172 influence the material's melting temperature, as found in (Dong *et al.*, 2011).

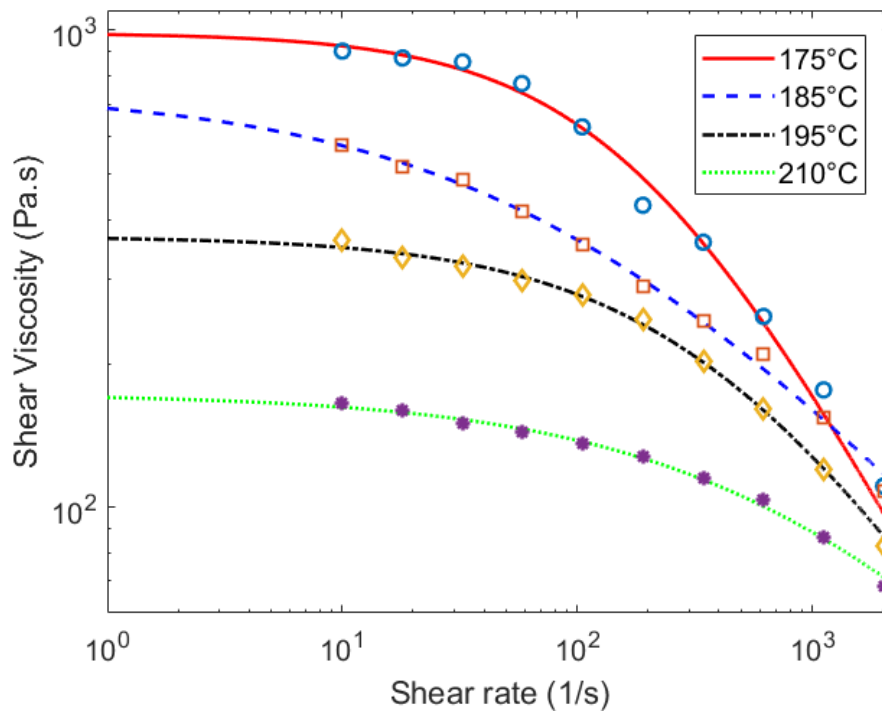
173 The PLA / HNT compounds' degradation temperatures were between  $318$  and  $326^\circ\text{C}$ ,  
174 values similar to those obtained from PLA / MWCNT nanocomposites, showing that  
175 halloysite nanotubes do not affect the degradation temperature.

176 *Capillary Rheometry Testing*

177 The tests were rehearsed at temperatures of  $175$ ,  $185$ ,  $195$ ,  $205$  and  $210^\circ\text{C}$  to observe  
178 the influence of nanocharges on the cutting speed of the material (flow resistance),  
179 which has a practical effect on polymer transformation processes.

180 Curve fitting was performed on MatLab software with the capillary rheometry data to  
181 determine the Cross WLF parameters.

182 The rheological behaviour curves of neat PLA at different temperatures show that PLA  
183 viscosity (flow resistance) decreases as the temperature of the material increases (see  
184 Fig. 4).



185

186

187

**Figure 4. Variation of melt viscosity with shear rates for neat PLA.**

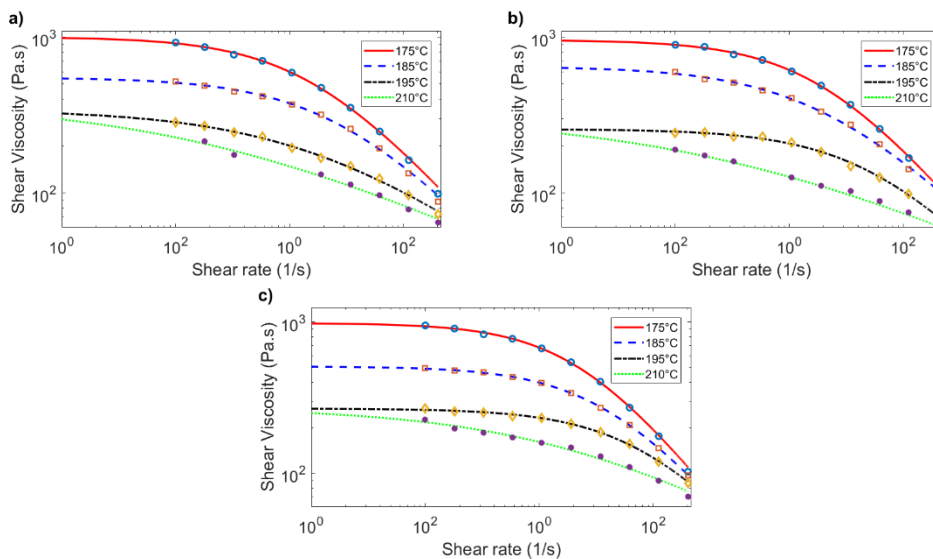
188

189

190

191

Figure 5 shows shear viscosity versus shear rate graphs for PLA / MWCNT nanocomposites at different rate (1/s). As shear stress increases the viscosity of the material decreases, showing the typical behaviour of a non-Newtonian pseudo-plastic material (Hamad, Kaseem and Deri, 2011)



192

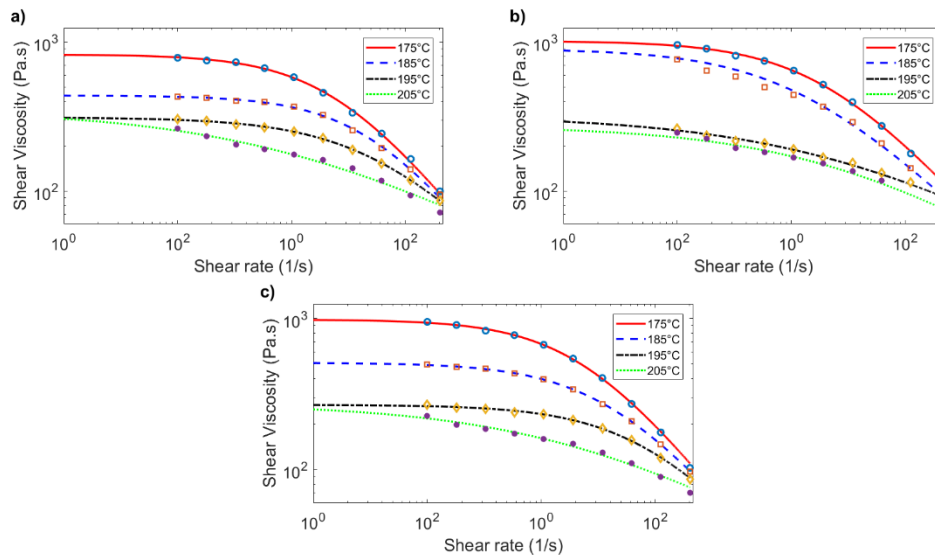
193 **Figure 5. Variation of shear viscosity with shear rate for PLA/MWCNT blends.**

194 a) PLA/0.5 wt.% MWCNTs, b) PLA/0.75 wt. % MWCNTs, c) PLA/1 wt. % MWCNTs.

195

196 When the temperature of the nanocomposites goes above 175 ° C the material does not  
197 offer greater flow resistance, and viscosity is the same as neat PLA, due to the influence  
198 of the carbon nanotubes. No appreciable difference in viscosity was found among the  
199 PLA / 0.5, 0.75 and 1% MWCNT nanocomposites, as was found between the neat PLA  
200 graph and that of the nanocomposites.

201 Figure 6 shows the shear viscosity graphs versus the PLA / HNT nanocomposites shear  
202 rate at different temperatures.



203

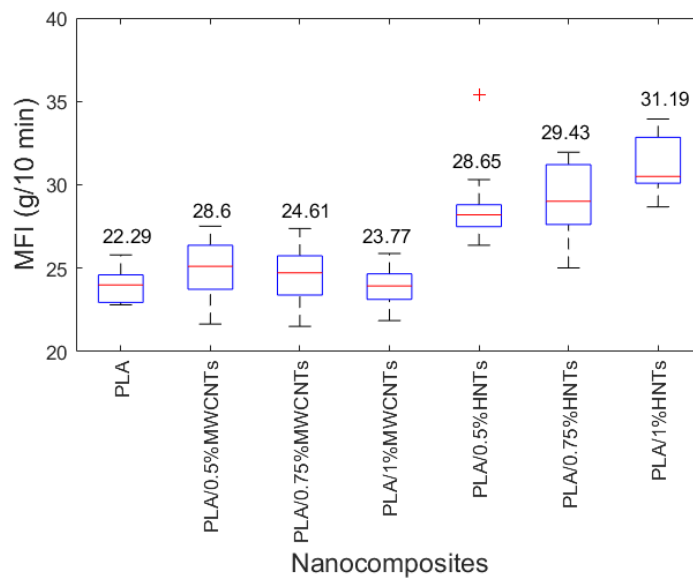
204 **Figure 6. Variation of shear viscosity with shear rate for PLA/HNT blends.**

205 a) PLA/0.5 wt.% HNTs, b) PLA/0.75 wt. % HNTs, c) PLA/1 wt. % HNTs.

206 As shown in Figure 6, as the percentage of halloysite nanotubes increases flow  
207 resistance decreases due to the poor stiffness of the nanotubes, which allows them to  
208 change direction with the flow, also due to the chain scission by hydrolysis, which  
209 reduces the viscosity of the nanocomposites (Singh *et al.*, 2016). It was not possible to  
210 test PLA / 1% HNTs at 210 ° C because the material flowed too fast to obtain any data,  
211 as was found in (Singh *et al.*, 2016)

212 *Melt Flow Index*

213 The melt flow index (MFI) properties of the neat PLA and the PLA / MWCNTs and  
214 PLA / HNTs nanocomposites were studied using a Melt Indexer 3000Q2 plastograph  
215 (Qualytest Instruments) under UNE-EN\_ISO\_1133.  
216 The MFI test on neat PLA, PLA / MWCNTs and PLA / HNTs carried out in load  
217 percentages of 0.5, 0.75 and 1% can be seen in Figure 7. Increasing the percentage of  
218 MWCNT reduced the MFI, which was the opposite with the HNT load.



219  
220 **Figure 7. The melt flow indexes (MFI) of neat PLA and nanocomposites of PLA /**  
221 **MWCNT and PLA / HNT with varying percentages of nanocharges.**

222 In Figure 7 it can be seen that MFI is reduced as the percentage of carbon nanotubes  
223 increases, probably due to the stiffness of the nanocharge, unlike the HNTs, whose MFI  
224 increases with higher nanocharges. This is probably due to the exfoliation / intercalation  
225 of a molecule or group, in this case assumed to be the water contained in the nanotubes,  
226 in agreement with the results obtained in (Li *et al.*, 2006).

227

228 The analysis of the behaviour of each of the nanocharges in the polymeric matrix  
229 indicates that the MWCNTs reduce their fluidity as the weight percentage increases,

230 while HNTs increase their fluidity as this percentage rises. The higher fluidity of these  
231 composite materials than that of neat PLA is due to the PLA degradation during  
232 extrusion caused by the cleavage of the PLA's oxygen chains (Ferri Azor, Balart  
233 Gimeno and Fenollar Gimeno, 2017), which involves the loss of molecular weight, as  
234 was found in (Li *et al.*, 2006).

## 235 **CONCLUSIONS**

236 PLA mixtures with MWCNTs and HNTs were obtained from a twin-screw cutting  
237 process to analyse the rheological properties of the materials for a future study of FDM  
238 applications.

239 A comparison of the results indicates that the variation of the glass transition  
240 temperature, melting temperature and degradation is within a range of 4 ° C.

241 A significant variation of 24 ° C was found in the crystallisation temperature, which was  
242 assumed to be due to the MWCNTs' higher thermal conductivity, unlike halloysite.

243 PLA / MWCNT viscosity values increase due to the division of the PLA chain by  
244 hydrolysis. PLA / HNT viscosity increases considerably with the inclusion of halloysite  
245 nanotubes, due to the excision present in the extrusion process, taking into account that  
246 halloysite is a material that absorbs humidity.

247 As the MFI values confirm the results of the capillary rheometry, it can be concluded  
248 that the nanomaterials studied could be used in FDM and Injection Moulding Processes.

249

## 250 **REFERENCES**

251 Angel Herráez (2011) 'Las asombrosas estructuras del carbono: fullerenos, grafenos y  
252 nanotubos', *Apuntes de Ciencias*, pp. 25–25.

253 Auras, R. A. *et al.* (2011) *Poly (lactic acid): synthesis, structures, properties,*  
254 *processing, and applications.*

255 Carrasco, F. *et al.* (2010) ‘Processing of poly(lactic acid): Characterization of chemical  
256 structure, thermal stability and mechanical properties’, *Polymer Degradation and*  
257 *Stability*. Elsevier, 95(2), pp. 116–125. doi:  
258 10.1016/J.POLYMDEGRADSTAB.2009.11.045.

259 Dong, Y. *et al.* (2011) ‘Development and characterisation of novel electrospun  
260 polylactic acid/tubular clay nanocomposites’, *Journal of Materials Science*, 46(18), pp.  
261 6148–6153. doi: 10.1007/s10853-011-5605-6.

262 Ferri Azor, J. M. ., Balart Gimeno, A. R. and Fenollar Gimeno, O. (2017) ‘Desarrollo de  
263 formulaciones derivadas de ácido poliláctico (PLA), mediante plastificación e  
264 incorporación de aditivos de origen natural’. Available at:  
265 [https://m.riunet.upv.es/bitstream/handle/10251/86166/Ferri - Desarrollo de](https://m.riunet.upv.es/bitstream/handle/10251/86166/Ferri%20-%20Desarrollo%20de%20formulaciones%20derivadas%20de%20ácido%20poliláctico%20PLA%20mediante%20plastificación....pdf?sequence=1&isAllowed=y)  
266 [formulaciones derivadas de ácido poliláctico %28PLA%29%2C mediante](https://m.riunet.upv.es/bitstream/handle/10251/86166/Ferri%20-%20Desarrollo%20de%20formulaciones%20derivadas%20de%20ácido%20poliláctico%20PLA%20mediante%20plastificación....pdf?sequence=1&isAllowed=y)  
267 [plastificación....pdf?sequence=1&isAllowed=y](https://m.riunet.upv.es/bitstream/handle/10251/86166/Ferri%20-%20Desarrollo%20de%20formulaciones%20derivadas%20de%20ácido%20poliláctico%20PLA%20mediante%20plastificación....pdf?sequence=1&isAllowed=y) (Accessed: 18 July 2018).

268 Gao, Y. *et al.* (2017) ‘Influence of filler size on the properties of poly(lactic acid)  
269 (PLA)/graphene nanoplatelet (GNP) nanocomposites’, *European Polymer Journal*, 86,  
270 pp. 117–131. doi: 10.1016/j.eurpolymj.2016.10.045.

271 Hamad, K., Kaseem, M. and Deri, F. (2011) ‘Melt Rheology of Poly(Lactic Acid)/Low  
272 Density Polyethylene Polymer Blends’, *Advances in Chemical Engineering and*  
273 *Science*. Scientific Research Publishing, 01(04), pp. 208–214. doi:  
274 10.4236/aces.2011.14030.

275 Harris, A. M. and Lee, E. C. (2008) ‘Improving mechanical performance of injection  
276 molded PLA by controlling crystallinity’, *Journal of Applied Polymer Science*. Wiley  
277 Subscription Services, Inc., A Wiley Company, 107(4), pp. 2246–2255. doi:  
278 10.1002/app.27261.

279 Kim, S. Y. *et al.* (2010) ‘Unique crystallization behavior of multi-walled carbon  
280 nanotube filled poly(lactic acid)’, *Fibers and Polymers*. The Korean Fiber Society,  
281 11(7), pp. 1018–1023. doi: 10.1007/s12221-010-1018-4.

282 Li, T. *et al.* (2006) ‘Polylactide, nanoclay, and core–shell rubber composites’, *Polymer*  
283 *Engineering & Science*. Wiley-Blackwell, 46(10), pp. 1419–1427. doi:  
284 10.1002/pen.20629.

285 López, J. *et al.* (2009) ‘Analysis weld seam weak in blow molding large parts made of  
286 commodity plastics’, *Engineering Failure Analysis*, 16(3), pp. 856–862. doi:  
287 10.1016/j.engfailanal.2008.07.007.

288 Murariu, M. and Dubois, P. (2016) ‘PLA composites: From production to properties’,  
289 *Advanced Drug Delivery Reviews*. Elsevier, 107, pp. 17–46. doi:  
290 10.1016/J.ADDR.2016.04.003.

291 Raquez, J.-M. *et al.* (2013) ‘Polylactide (PLA)-based nanocomposites’, *Progress in*  
292 *Polymer Science*, 38(10–11), pp. 1504–1542. doi: 10.1016/j.progpolymsci.2013.05.014.

293 Ren, J. (2011) *Biodegradable poly (lactic acid): synthesis, modification, processing and*  
294 *applications*.

295 Richard, T. (2008) ‘Preparación y caracterización de nanocompuestos en base PLA’.  
296 Universitat Politècnica de Catalunya. Available at:  
297 <http://upcommons.upc.edu/handle/2099.1/4791> (Accessed: 26 July 2017).

298 Singh, V. P. *et al.* (2016) ‘High-density polyethylene/halloysite nanocomposites:  
299 morphology and rheological behaviour under extensional and shear flow’, *Journal of*  
300 *Polymer Research*. Springer Netherlands, 23(3), p. 43. doi: 10.1007/s10965-016-0937-  
301 1.



302 Song, Y. *et al.* (2017) ‘Measurements of the mechanical response of unidirectional 3D-  
303 printed PLA’, *Materials & Design*. Elsevier, 123, pp. 154–164. doi:  
304 10.1016/J.MATDES.2017.03.051.

305 Suriñach, S. *et al.* (1992) ‘La calorimetría diferencial de barrido y su aplicación a la  
306 Ciencia de Materiales’, 31. Available at: <http://boletines.secv.es/upload/199231011.pdf>  
307 (Accessed: 26 July 2017).

308 Wu, W. *et al.* (2013) ‘Polylactide/halloysite nanotube nanocomposites: Thermal,  
309 mechanical properties, and foam processing’, *Journal of Applied Polymer Science*,  
310 130(1), pp. 443–452. doi: 10.1002/app.39179.

311 Yuan, P., Tan, D. and Annabi-Bergaya, F. (2015) ‘Properties and applications of  
312 halloysite nanotubes: Recent research advances and future prospects’, *Applied Clay*  
313 *Science*, pp. 75–93. doi: 10.1016/j.clay.2015.05.001.

314